DNA Repair 80 (2019) 52–58

Contents lists available at ScienceDirect

DNA Repair

journal homepage: www.elsevier.com/locate/dnarepair

High levels of oxidatively generated DNA damage 8,5′-cyclo-2′-deoxyadenosine accumulate in the brain tissues of xeroderma pigmentosum group A gene-knockout mice

Toshio Mori[a,b,*], Hironobu Nakane[c], Takaaki Iwamoto[a,b], Marios G. Krokidis[d,e], Chryssostomos Chatgilialoglu[d], Kiyoji Tanaka[f], Toshiyuki Kaidoh[c], Masatoshi Hasegawa[a], Shigeki Sugiura[g]

[a] Department of Radiation Oncology, Nara Medical University, Kashihara, Nara, 634-8521, Japan
[b] Radioisotope Research Center, Nara Medical University, Kashihara, Nara, 634-8521, Japan
[c] Department of Anatomy, Faculty of Medicine, Tottori University, Yonago, Tottori, 683-8503, Japan
[d] ISOF, Consiglio Nazionale delle Ricerche, Bologna, Italy
[e] Institute of Nanoscience and Nanotechnology, NSCR "Demokritos", Athens, Greece
[f] Graduate School of Frontier Biosciences, Osaka University, Suita, Osaka, 565-0871, Japan
[g] Medical Genetics Research Center, Nara Medical University, Kashihara, Nara, 634-8521, Japan

ARTICLE INFO

Keywords:
Xeroderma pigmentosum
Neurodegeneration
Oxidatively generated DNA damage
Nucleotide excision repair
Xpa knockout mice

ABSTRACT

Xeroderma pigmentosum (XP) is a genetic disorder associated with defects in nucleotide excision repair, a pathway that eliminates a wide variety of helix-distorting DNA lesions, including ultraviolet-induced pyrimidine dimers. In addition to skin diseases in sun-exposed areas, approximately 25% of XP patients develop progressive neurological disease, which has been hypothesized to be associated with the accumulation of an oxidatively generated type of DNA damage called purine 8,5′-cyclo-2′-deoxynucleoside (cyclopurine). However, that hypothesis has not been verified. In this study, we tested that hypothesis by using the XP group A gene-knockout ($Xpa^{-/-}$) mouse model. To quantify cyclopurine lesions in this model, we previously established an enzyme-linked immunosorbent assay (ELISA) using a monoclonal antibody (CdA-1) that specifically recognizes 8,5′-cyclo-2′-deoxyadenosine (cyclo-dA). By optimizing conditions, we increased the ELISA sensitivity to a detection limit of ~one cyclo-dA lesion/10^6 nucleosides. The improved ELISA revealed that cyclo-dA lesions accumulate with age in the brain tissues of $Xpa^{-/-}$ and of wild-type (wt) mice, but there were significantly more cyclo-dA lesions in $Xpa^{-/-}$ mice than in wt mice at 6, 24 and 29 months of age. These findings are consistent with the long-standing hypothesis that the age-dependent accumulation of endogenous cyclopurine lesions in the brain may be critical for XP neurological abnormalities.

1. Introduction

Xeroderma pigmentosum (XP) is an autosomal recessive genetic disorder associated with defects in the nucleotide excision repair (NER) pathway, which eliminates a wide variety of helix-distorting types of DNA damage including ultraviolet (UV)-induced pyrimidine dimers, such as cyclobutane pyrimidine dimers (CPDs) and (6-4) photoproducts, and bulky chemical adducts [1,2]. XP is characterized by extreme UV sensitivity, abnormal skin pigmentation and an increased incidence of sunlight-induced skin cancers [3–5]. There are seven different genetic complementation groups of XP (XP-A to XP-G) and a variant form [12]. Importantly, about 25% of XP patients develop progressive neurological abnormalities (XP neurological disease), with a considerably higher rate in Japan [6–9]. The most severe and earliest onset cases of XP neurological disease are seen in XP-A patients [10]. The symptoms of XP neurological disease include peripheral neuropathy, sensory deafness, spasticity, cerebellar ataxia, mental deterioration and microcephaly [11]. Those neurological abnormalities are

Abbreviations: cyclopurine, purine 8,5′-cyclo-2′-deoxynucleoside; cyclo-dA, 8,5′-cyclo-2′-deoxyadenosine; cyclo-dG, 8,5′-cyclo-2′-deoxyguanosine; $Xpa^{-/-}$ mouse, xeroderma pigmentosum group A gene-knockout mouse; LC–MS/MS, liquid chromatography-tandem mass spectrometry; ELISA, enzyme-linked immunosorbent assay

* Corresponding author: Department of Radiation Oncology, Nara Medical University, Kashihara, Nara, 634-8521, Japan.
E-mail address: tmori@naramed-u.ac.jp (T. Mori).

https://doi.org/10.1016/j.dnarep.2019.04.004
Received 14 January 2019; Received in revised form 27 February 2019; Accepted 12 April 2019
Available online 13 April 2019

caused by the primary degeneration of normally developed neurons with resultant axonopathy and widespread gliosis [12,13]. However, the mechanism(s) underlying the development of XP neurological disease remains obscure [14,15].

More than 40 years ago, Andrews et al. [10] reported that XP neurological abnormalities correlate with colony-forming ability after UV radiation using fibroblast strains derived from 24 XP patients. They hypothesized that since UV radiation from the sun cannot penetrate the skull, some types of endogenous DNA damage may arise in the brain that are normally repaired by the NER pathway. In the absence of NER, this postulated damage would accumulate and ultimately lead to neuronal death due to the decreased expression of essential genes and result in XP neurological disease. In 2000, two research groups [16,17] reported a class of oxidatively generated DNA damage called purine 8,5′-cyclo-2′-deoxynucleosides (cyclopurines) that are indeed substrates exclusively for NER [16,17]. Further, it was demonstrated that these lesions strongly block gene expression in mammalian cells [16,18–21]. Cyclopurine lesions are formed by the attack of hydroxyl radicals on DNA and specifically on 2′-deoxyadenosine and 2′-deoxyguanosine [22]. Hydroxyl radicals react with sugar moieties by abstracting an H atom from C5′, resulting in the formation of the C5′ radical. The C5′ radical attacks the double bond between N7 and C8 of purine bases, ultimately resulting in the formation of a covalent 8,5′-bond. Both 8,5′-cyclo-2′-deoxyadenosine (cyclo-dA) and 8,5′-cyclo-2′-deoxyguanosine (cyclo-dG) can exist in either of two diastereomers, denoted 5′*R* and 5′*S* [23,24]. Cyclopurines can be induced in DNA by gamma irradiation under anoxic conditions [25–27] or by transition metal ion-mediated Fenton reactions [28,29]. Importantly, they are formed endogenously in cellular DNA of mammals including humans [30–33] and are chemically very stable [34,35]. Thus, since cyclopurine lesions fulfill the criteria for candidates of DNA lesions in the hypothesis regarding the cause of XP neurological disease, the essential task for testing that hypothesis is to demonstrate that more cyclopurine lesions accumulate with age in brain tissues from XP patients or from XP mice than from their controls. However, such evidence has not been provided, even though several groups have actively quantified those lesions using a liquid chromatography-tandem mass spectrometry (LC−MS/MS) coupled with isotope-dilution technique [27,33,36–38].

To test the hypothesis, we used XP group A gene-knockout ($Xpa^{-/-}$) mice that are defective in NER and are highly susceptible to UV-B- or chemical-induced skin carcinogenesis [39]. Moreover, since a sensitive method capable of measuring small amounts of endogenous cyclopurine lesions was needed, we generated a monoclonal antibody (CdA-1) that is specific for cyclo-dA (including both 5′*R*-cyclo-dA and 5′*S*-cyclo-dA) in DNA [23] and used it in an enzyme-linked immunosorbent assay (ELISA) for the quantification of cyclo-dA. However, the detection level of the ELISA was as low as ~10 cyclo-dA lesions/10^6 nucleosides in 0.5 μg DNA sample, and therefore was not sufficient to discriminate the accumulation levels of cyclo-dA in tissues between $Xpa^{-/-}$ and control wild-type (wt) mice.

In the present study, we first made efforts to increase the ELISA sensitivity by optimizing several conditions. Then, to test the hypothesis for the development of XP neurological disease, we used the improved ELISA to investigate whether more cyclo-dA lesions accumulate with age in the brain tissues of $Xpa^{-/-}$ mice compared to wt mice. We also examined age-related accumulations of cyclo-dA in liver, kidney and testis in $Xpa^{-/-}$ and in wt mice for comparison.

2. Materials and methods

2.1. Chemicals

A 20-mer oligonucleotide containing a single 5′*S*-cyclo-dA (5′*S*-cyclo-dA-oligo; 5′-TCTCCCN**X**NGCGTGCGCCTT-3′) (where **X** is 5′*S*-cyclo-dA and N is either A, C, G or T) and a corresponding control oligonucleotide (control oligo) were purchased from Hokkaido System Science (Sapporo, Japan). Calf thymus DNA (ctDNA) and bovine serum albumin (BSA) were purchased from Sigma-Aldrich (St. Louis, MO). The ctDNA treated with Fenton-type reagents (Fenton DNA) was prepared by incubation for 24 h with 100 μM $CuCl_2$, 800 μM H_2O_2 and 8 mM ascorbate as described previously [23].

2.2. Mice

All animal experiments in this study were conducted according to the guidelines for the institutional animal care and use committee and the safety committee for genetic recombination experiments of Tottori University. *Xpa* gene-knockout ($Xpa^{-/-}$) mice were generated by insertion of the *neo* gene into exon 4 of the mouse *Xpa* gene [39], and had a chimeric genetic background of CBA/C57BL6/CD-1. $Xpa^{-/-}$ and wt mice were kept under specific pathogen-free conditions, housed in a controlled environment at 20–26 °C, fed a CE-2 diet (Clea Japan Inc, Tokyo, Japan) and sterilized water ad libitum.

2.3. Liquid chromatography isotope dilution tandem mass spectrometry (LC–MS/MS) analysis

The levels of cyclopurine lesions in untreated ctDNA were quantified by using isotope dilution LC–MS/MS analysis as described previously [40,41].

2.4. Enzyme-linked immunosorbent assay (ELISA)

The level of cyclo-dA in each DNA sample was measured by a sensitive direct ELISA using the CdA-1 antibody as described previously [23] with some modifications. The modified ELISA method was the same as before, except that : (1) the coating amount of single-stranded DNA sample was increased to 1 μg per well, (2) CdA-1 antibody diluted 1:30,000 in 10 mM PBS (0.14 M NaCl, pH 7.4) was used, (3) goat anti-mouse IgG (H + L) conjugated to biotin, $F(ab')_2$ fragment (diluted 1:500 in PBS; Rockland Immunochemicals, Limerick, PA) was used, (4) streptavidin-polyHRP80 (diluted 1:5000 in PBS containing 3% BSA and 1% Tween-20; STD, Baesweiler, Germany) was used.

2.5. Generation of a standard dose-response curve

Oligonucleotide samples containing various amounts of 5′*S*-cyclo-dA (1–50 lesions/10^6 nucleosides) were prepared by mixing 5′*S*-cyclo-dA-oligo and unmodified control oligo in different ratios. After coating the samples on plates, the improved ELISA with the CdA-1 antibody was performed to generate a standard dose-response curve between the amount of 5′*S*-cyclo-dA and the antibody binding to them. A standard curve was generated in each ELISA experiment to calculate the absolute amounts of cyclo-dA.

2.6. Quantification of cyclo-dA in DNA from mouse tissues

$Xpa^{-/-}$ and wt mice were sacrificed by cervical dislocation at ages of 1, 3, 6, 24 or 29 months, and their tissues, including the brain, liver, kidneys and testes, were removed, soaked in liquid nitrogen and stored at −80 °C until processed. Genomic DNA was then purified using a DNA Extractor TIS Kit (Wako Pure Chemical, Osaka, Japan) according to the manufacturer's protocol. DNA samples from mouse tissues and untreated ctDNA were heat-denatured, coated on the same plate, and then their binding of antibody (OD492 value) was measured by the improved ELISA. The absolute amounts of cyclo-dA lesions in individual DNA samples were calculated from their OD492 values, after subtracting the OD492 value of ctDNA, using the standard dose-response curve obtained from the same plate. In cases where the standard curve was not obtained correctly, possibly because of detachment of oligo samples from the plate, we used an average standard curve consisting of 23 typical standard curves that had been collected from the ELISA

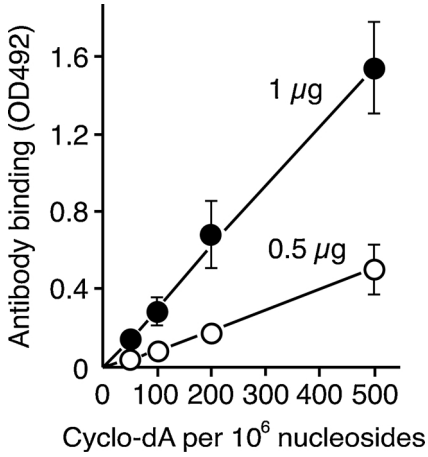

Fig. 1. Increase in ELISA sensitivity for the detection of cyclo-dA by increasing the amount of sample DNA coated on the plate. CdA-1 binding to cyclo-dA was compared between 0.5 and 1 μg/well oligonucleotides containing various amounts of cyclo-dA using the ELISA with CdA-1 (diluted 1:10,000 in a high salt buffer). Each point shows the mean (± SD) of three experiments.

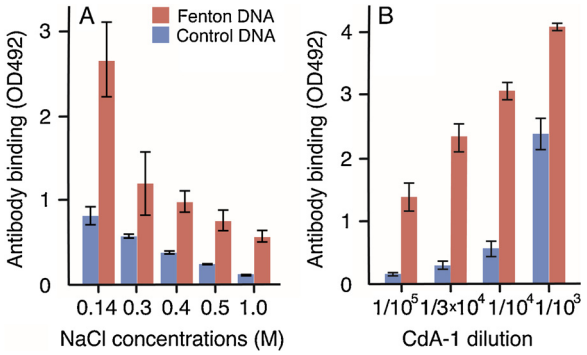

Fig. 2. Increase in ELISA sensitivity to detect cyclo-dA by employing a low salt buffer with a more diluted CdA-1 antibody. (A) Levels of CdA-1 binding to Fenton DNA (˜200 cyclo-dA lesions/10^6 nucleosides) [23] and to control DNA were measured by ELISA using CdA-1 (diluted 1:10,000) containing buffer with different NaCl concentrations. Each bar shows the mean (± SD) of three experiments. (B) Levels of CdA-1 binding to Fenton DNA and to control DNA were measured by ELISA using 0.14 M NaCl buffer with different dilutions of CdA-1. Each bar shows the mean (± SD) of three experiments.

experiments in this study.

3. Results

3.1. Optimization of the sensitivity of the ELISA for cyclo-dA detection

We previously established an ELISA for cyclo-dA with a detection limit of ˜10 cyclo-dA lesions/10^6 nucleosides in a 0.5 μg DNA sample [23]. However, since that detection sensitivity was not sufficient to discriminate the accumulated levels of cyclo-dA in tissues between *Xpa*$^{-/-}$ and wt mice, we increased the ELISA sensitivity by optimizing several conditions. Fig. 1 shows the effects of doubling the coating amount of DNA from 0.5 to 1 μg/well on the sensitivity of the ELISA. In both coating conditions, linear dose-response curves between the amounts of cyclo-dA and the antibody binding to them were obtained. As expected, 1 μg DNA coating produced 3-fold higher signals than the original 0.5 μg coating.

Since the CdA-1 antibody has the ability to bind cyclo-dA in DNA, it has some affinity for DNA itself, in addition to its strong affinity for the lesion. In the original ELISA [23], a high salt (0.5 M NaCl) buffer was used to reduce the affinity of CdA-1 for DNA, but it resulted in lowering the affinity for cyclo-dA in DNA at the same time. Thus, we investigated the best combination of NaCl concentration in the buffer and the dilution of CdA-1 to increase the ELISA sensitivity. We initially measured the levels of CdA-1 binding to Fenton DNA and to control DNA using CdA-1 (diluted 1:10,000) in buffer with different NaCl concentrations (Fig. 2A). Both levels increased with decreasing NaCl concentrations, with the highest binding at 0.14 M NaCl. To identify the optimal dilution of CdA-1 which produces high binding to cyclo-dA but low binding to DNA, we performed the ELISA using 0.14 M NaCl buffer with different dilutions of CdA-1 (Fig. 2B). We found that a CdA-1 dilution of 1/30,000 is adequate for this purpose. The combination of CdA-1 diluted at 1:30,000 and the buffer with 0.14 M NaCl increased the ELISA sensitivity more than 3 times. We could not find any further effective alterations to improve the ELISA sensitivity.

After incorporating those optimal conditions (shown in Figs. 1 and 2) into the ELISA, we generated a new dose-response curve (Fig. 3). The linear dose-response curve suggests that the CdA-1's specificity toward cyclo-dA has been preserved in new conditions. The improved ELISA produced a ten-fold increase in sensitivity compared to the original ELISA with a detection limit of ˜one cyclo-dA lesion/10^6 nucleosides in a 1 μg DNA sample.

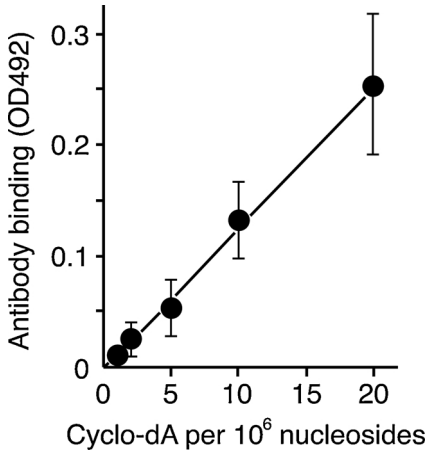

Fig. 3. Ten-fold increase in sensitivity for the detection of cyclo-dA using the improved ELISA. The binding of CdA-1 to cyclo-dA was measured on oligo samples containing various amounts of cyclo-dA using the improved ELISA, which includes DNA coating with 1 μg/well and CdA-1 treatment with a 1/30,000 dilution in a low salt (0.14 M NaCl) buffer. Each point shows the mean (± SD) of three experiments.

3.2. Quantification of cyclopurine lesions in ctDNA by LC–MS/MS analysis

Isotope dilution LC–MS/MS analysis revealed that the levels (lesions/10^6 nucleosides) of 5′*R*-cyclo-dA, 5′*S*-cyclo-dA, 5′*R*-cyclo-dG and 5′*S*-cyclo-dG in untreated ctDNA are 0.43 ± 0.15, 0.00 ± 0.00, 7.79 ± 2.51 and 3.74 ± 1.18, respectively. Those numbers represent the means (± SD) of n = 4 independent experiments. Thus, our ctDNA contained 0.43 cyclo-dA lesions/10^6 nucleosides. When cellular DNA damage (for example, UV-induced DNA damage) is measured by ELISA, the difference in levels of antibody binding to antigen between UV-irradiated DNA and unirradiated control DNA is utilized for calculation of the lesion levels. However, since cyclo-dA is endogenously produced in cellular DNA, there is no proper control DNA like unirradiated DNA. In this study, we chose untreated ctDNA as control DNA, because it contains only 0.43 cyclo-dA lesions/10^6 nucleosides, which is below the detection limit of the improved ELISA. The control DNA was fully utilized for the calculation of cyclo-dA levels in mouse tissues.

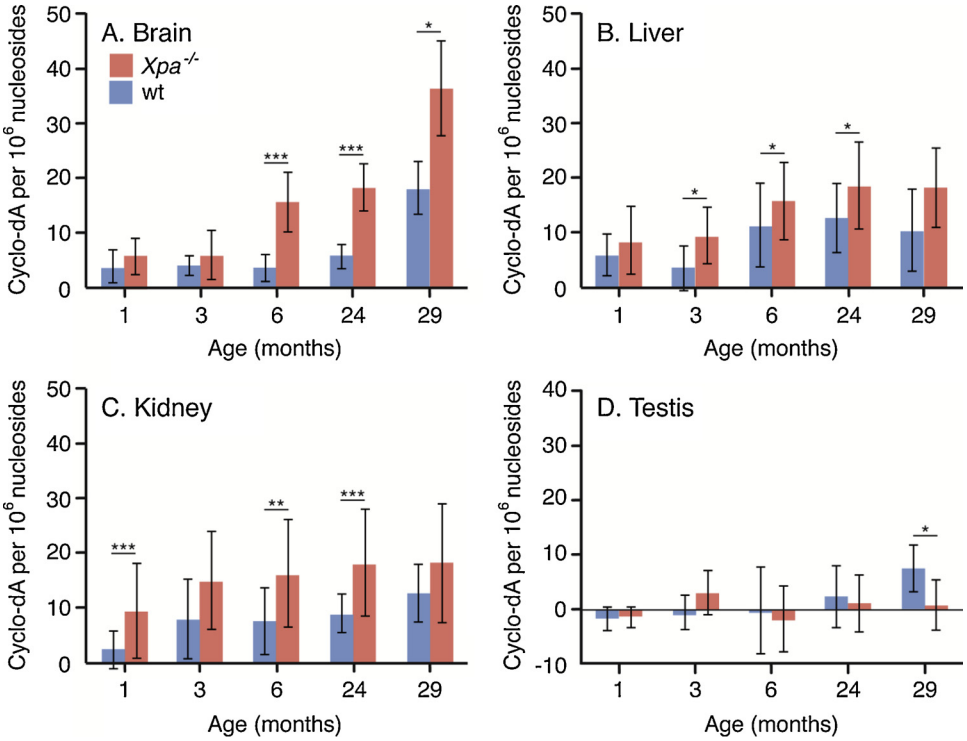

Fig. 4. Levels of cyclo-dA in the brain, liver, kidney and testis from *Xpa*$^{-/-}$ and from wt mice at various ages. Using the improved ELISA, cyclo-dA levels in genomic DNA from the brain (A), liver (B), kidney (C) and testis (D) from *Xpa*$^{-/-}$ and from wt mice aged from 1 to 29 months were measured. The data represent means (± SD) of the measurement results. The numbers of mice and measurements for each data point are shown in Table 1. *p* values were calculated using an unpaired two-tailed Student's *t* test. *, $p < 0.05$; **, $p < 0.01$; ***, $p < 0.001$.

3.3. Quantification of cyclo-dA lesions in tissues of Xpa$^{-/-}$ *and of wt mice at various ages*

With the improved ELISA, we measured the levels of cyclo-dA in genomic DNAs from brain, liver, kidney and testis from *Xpa*$^{-/-}$ and from wt mice aged from 1 to 29 months (Fig. 4). For each data point, 3 different mice were used (with some exceptions), and ELISA measurements were repeated many times to obtain the most reliable results. Details of those measurements are shown in Table 1.

In the brain (Fig. 4A), cyclo-dA lesions indeed accumulated with age in DNAs of *Xpa*$^{-/-}$ and of wt mice. The cyclo-dA levels were 5.9 and 3.8 lesions per 10^6 nucleosides at 1 month of age, and 36.3 and 18.1 lesions per 10^6 nucleosides at 29 months of age in *Xpa*$^{-/-}$ and in wt mice, respectively. Remarkably, there were significantly more cyclo-dA lesions in *Xpa*$^{-/-}$ mice than in wt mice at 6, 24 and 29 months of age. Moreover, the level of cyclo-dA in the brain of 29-month-old *Xpa*$^{-/-}$ mouse was highest of the 4 tissues examined. These results are in line with the hypothesis for the development of XP neurological disease.

In the liver (Fig. 4B) and kidney (Fig. 4C), cyclo-dA lesions accumulated in DNAs of *Xpa*$^{-/-}$ and of wt mice in an age-dependent manner with consistently higher levels in *Xpa*$^{-/-}$ mice, which is consistent with the results of the brain. However, differences in the levels of cyclo-dA between *Xpa*$^{-/-}$ and wt mice at 6, 24 and 29 months of age were much smaller in the liver (4.5, 5.8 and 7.8 lesions per 10^6 nucleosides) and kidney (8.6, 9.1 and 5.5 lesions per 10^6 nucleosides) than in the brain (12.3, 12.7 and 18.2 lesions per 10^6 nucleosides), respectively. These results indicate that the improved ELISA is sufficiently sensitive to measure cyclo-dA levels in tissues of *Xpa*$^{-/-}$ and of wt mice.

In the testis (Fig. 4D), in contrast to the other 3 tissues, very low accumulations of cyclo-dA were observed both in *Xpa*$^{-/-}$ and in wt mice aged from 1 to 29 months. The levels of cyclo-dA were not significantly different between *Xpa*$^{-/-}$ and wt mice except at 29 months of age. Interestingly, the levels of cyclo-dA in wt mice were higher than *Xpa*$^{-/-}$ mice at 24 and 29 months of age. This indicates that the pattern of age-related accumulation of cyclo-dA is tissue-specific.

4. Discussion

4.1. Mechanism(s) underlying the development of XP neurological disease

In the present study, we tested the hypothesis that XP neurological

Table 1
Summary of ELISA measurements in mouse tissues.

		Brain		Liver		Kidney		Testis	
	Age (months)	Total No of mice	Total No of measurements	Total No of mice	Total No of measurements	Total No of mice	Total No of measurements	Total No of mice	Total No of measurements
Xpa$^{-/-}$	1	3	18	3	18	3	18	3	9
	3	3	18	3	18	3	18	3	9
	6	3	9	3	24	3	18	3	18
	24	3	9	2	16	3	18	3	18
	29	1	3	1	8	1	6	1	6
wt	1	3	18	3	18	3	18	3	9
	3	1	6	1	6	1	6	1	3
	6	3	9	3	24	3	18	3	18
	24	3	9	3	24	3	18	3	18
	29	1	3	1	8	1	6	1	6

disease is associated with the accumulation of cyclopurines using the *Xpa*$^{-/-}$ mouse model. To quantify cyclopurine lesions, we previously established an ELISA with the CdA-1 antibody that can measure the level of cyclo-dA, including both the 5′*S* and the 5′*R* diastereomers. Moreover, by optimizing conditions, including the coating amount of DNA sample, the concentration of CdA-1 and the NaCl concentration in the buffer, we succeeded in increasing the ELISA sensitivity 10 times with a detection limit of ˜one cyclo-dA/10^6 nucleosides in a 1 μg DNA sample. Fortunately, this improved ELISA enabled us to determine the accumulation levels of cyclo-dA in tissues of *Xpa*$^{-/-}$ and of wt mice. In the brain, cyclo-dA lesions accumulated with age in genomic DNA of *Xpa*$^{-/-}$ and of wt mice, but there were significantly more cyclo-dA lesions in *Xpa*$^{-/-}$ mice than in wt mice at 6, 24 and 29 months of age. Moreover, the level of cyclo-dA in the brain of 29-month-old *Xpa*$^{-/-}$ mouse was highest of the 4 tissues examined. Thus, cyclopurine lesions fulfill the criteria for candidate factors that cause DNA lesions in the hypothesis regarding XP neurological disease, including: 1) substrates exclusively for NER, 2) block transcription, 3) endogenous DNA lesions, and 4) chemically stable DNA lesions. These findings based on the *Xpa*$^{-/-}$ mouse model are consistent with the long-standing hypothesis that the age-dependent accumulation of cyclopurine lesions in the brain may be critical for XP neurological disease. To further validate that hypothesis, it is necessary to confirm the accumulation of higher levels of cyclo-dA lesions in neurons of brain tissues from *Xpa*$^{-/-}$ mice than from wt mice.

There has been a report investigating cyclopurine levels at different ages in NER-deficient *Ercc1*$^{-/\Delta}$and in wt mice [33]. In the liver, cyclopurine levels increased with age in wt mice, and were dramatically higher in age-matched *Ercc1*$^{-/\Delta}$ mice. However, in the brain, there were no age-dependent increases in the levels of most cyclopurine lesions in *Ercc1*$^{-/\Delta}$ and in wt mice, maintaining constant levels such as 0.1-0.2 lesions/10^6 nucleosides. Since Ercc1 protein is involved in the repair of DNA interstrand crosslinks and some double-strand breaks, in addition to NER, the low levels of lesions in *Ercc1*$^{-/\Delta}$ mice were interpreted as possibly reflecting neuronal loss that has been shown to occur in the brain of those animals [42,15]. However, the results in the brain of wt mice, which is not damaged, are inconsistent with our study. The different results provided by the different methods are discussed later.

Recently, it was reported that the neurodegeneration of XP-A patients may be associated with mitochondrial and mitophagic dysfunction through PARP-1 hyperactivation and NAD$^+$/SIRT1 reduction [14]. That study suggested that this pathogenesis appears common to ataxia-telangiectasia (AT) and Cockayne syndrome (CS), two other DNA repair disorders with neurodegeneration. However, this may be hard to accept as a primary mechanism, because there are major differences in neurodegeneration among XP-A, AT and CS patients [43]. Thus, it may be reasonable to consider that XP neurological disease is primarily associated with the accumulation of cyclopurine lesions and secondarily with mitochondrial and mitophagic dysfunction.

Xpa$^{-/-}$ mice are known not to develop any detectable neurodegeneration, in contrast to human XP-A patients, although they are defective in NER and are highly susceptible to UV-B-induced skin carcinogenesis [39,44–46]. The earliest clinical signs of the presence of XP neurological disease are diminished or absent deep tendon reflexes and high frequency hearing loss [5]. Indeed, after 6 years of age, XP-A patients gradually develop areflexia, sensorineural hearing impairment and mental retardation [47]. These results suggest that it takes at least 6 years for the accumulated cyclopurine lesions to lead to extensive neuronal death and to XP neurological disease. If the rate of lesion formation and the mechanism of pathogenesis would not be largely different between humans and mice, one simple explanation is that the three-year life-span of *Xpa*$^{-/-}$ mice might be too short to develop neurodegeneration. However, it was recently reported that *Xpa*$^{-/-}$ mice aged 38–40 weeks exhibit sensorineural hearing loss, with significantly higher ABR (auditory brainstem response) thresholds at 4, 8 and 16 kHz than wt mice [48]. Further, the number of spiral ganglion neurons was reduced in *Xpa*$^{-/-}$ mice compared with wt mice, which suggests that the hearing loss is related to spiral ganglion neuron deficiency.

4.2. Differences in age-related cyclo-dA accumulation among mouse tissues

The patterns of age-dependent accumulation of cyclo-dA in *Xpa*$^{-/-}$ and in wt mice were different among the 4 tissues examined. In particular, the largest difference was observed between the brain and testis tissues. In the brain, as mentioned above, there were age-dependent accumulations with much higher levels of cyclo-dA in *Xpa*$^{-/-}$ mice than in wt mice, indicating that DNA repair (NER) functions steadily to eliminate cyclopurines from genomic DNA. This is consistent with evidence that post-mitotic neurons from humans and rodents as well as astrocytes from rodents have a reduced but substantial ability of global genome NER [49,50]. In contrast, in the testis, there were minimal accumulations at the time points assessed without significant differences in the levels of cyclo-dA between *Xpa*$^{-/-}$ and wt mice except at 29 months of age. Since all spermatogenic cell types have the ability of global genome NER [51], the very low cyclo-dA accumulations without significant differences between *Xpa*$^{-/-}$ and wt mice suggest that there is much more efficient cellular mechanism than DNA repair to reduce cyclopurine levels. Testes contain proliferating spermatogonia for spermatogenesis. Once a cell divides into two daughter cells, the level of DNA lesions in each daughter cell is theoretically reduced by half through DNA replication. Thus, DNA replication of proliferating cells may play a significant role in reducing the cyclo-dA levels in testis DNA irrespective of the NER ability of mice. However, it seems inconsistent that the levels of cyclo-dA in wt mice are higher than *Xpa*$^{-/-}$ mice at 24 and 29 months of age. In this context, we previously found a pronounced reduction in the weight and degenerative seminiferous tubules of the testes of *Xpa*$^{-/-}$ mice [44]. By the age of 24 months, almost all spermatogenic cells had degenerated in *Xpa*$^{-/-}$ mice but interstitial Leydig cells had proliferated. In contrast, essentially all seminiferous tubules were normal in wt mice even at the age of 24 months. It has been reported that the ability of global genome NER decreases with age in postmeiotic spermatogenic cells [51]. Thus, differences in the cellular composition of testes and the reduced NER ability in postmeiotic cells may be associated with the higher levels of cyclo-dA in wt mice than *Xpa*$^{-/-}$ mice at 24 and 29 months of age. Regarding the impaired spermatogenesis in *Xpa*$^{-/-}$ mice, this may be explained by the toxic effects of unrepaired cyclopurine lesions in spermatogenic cells being associated not only with transcription blockage but also with replication blockage. At sites of stalled replication forks, DNA double-strand breaks may arise and work as potent inducers of apoptosis [52]. In the liver and kidney, there were age-dependent accumulations similar to those of the brain, but the differences in levels of cyclo-dA between *Xpa*$^{-/-}$ and wt mice were much smaller in the liver and kidney than in the brain. The brain contains post-mitotic neurons, while the liver is an organ with high regenerative capacity [53]. This suggests that relatively more proliferating cells in the liver and kidney than in the brain may play a role in reducing those differences. Taken together, the present results suggest that steady-state cyclopurine levels in total genomic DNA of animal tissues are primarily determined by DNA repair (NER) and by DNA replication. This may explain why the basal levels of cyclopurines are very low in proliferating cultured mammalian cells [41].

4.3. Comparison of methods for cyclopurine quantification

It is worth comparing the cyclo-dA levels measured by our improved ELISA with other methods. The data by Wang and colleagues [33,38] may be a proper choice for comparison, because they measured the levels of cyclopurines in animal tissues using liquid chromatography-tandem mass spectrometry approach following an efficient enzymatic

digestion of DNA sample [40]. For example, the levels of 5′*R*-cyclo-dA and 5′*S*-cyclo-dA were 0.9 and 0.6 lesions per 10^6 nucleosides in the liver, and both were ~0.1 lesions per 10^6 nucleosides in the brain of 5-month-old wt mice [33]. Moreover, similar levels of 5′*R*-cyclo-dA and 5′*S*-cyclo-dA with ~0.1 lesions per 10^6 nucleosides were measured in both the liver and the brain of 3-month-old wt rats [38]. These levels are roughly one order of magnitude lower than our present results except those of the mouse liver. Recently however, a nanoflow liquid chromatography-nanoelectrospray ionization-tandem mass spectrometry (NanoLC-NSI-MS/MS) coupled with the isotope-dilution method was developed by the same group [54], which has a much higher sensitivity than the original LC—MS/MS. Interestingly, NanoLC-NSI-MS/MS analysis showed that the levels of 5′*S*-cyclo-dA are 1.2 and 1.5 lesions per 10^6 nucleosides in the liver and the brain of 4-month-old wt rats, respectively. Assuming that the levels of cyclo-dA are two-fold of 5′*S*-cyclo-dA levels, the cyclo-dA levels with 2.4 and 3.0 lesions per 10^6 nucleosides in the liver and the brain of rats are very similar to those with 3.5 and 4.1 lesions per 10^6 nucleosides in the liver and the brain of 3-month-old mice obtained in this study. Thus, it should be emphasized that cyclo-dA levels measured by the improved ELISA are comparable to those measured by the most sensitive NanoLC-NSI-MS/MS method.

Another attractive feature of immunoassays is that they can be used with immunofluorescence to detect DNA lesions within individual cells or tissues. Indeed, we could observe cyclo-dA as dots in 5′*S*-cyclo-dA-oligo-transfected human cells [23]. To further validate the hypothesis for the development of XP neurological disease, we are currently comparing the levels of cyclo-dA between neurons of the brain tissues from *Xpa*$^{-/-}$ and from wt mice using immunofluorescence with CdA-1.

5. Conclusions

We tested the hypothesis for the development of XP neurological disease by using the *Xpa*$^{-/-}$ mouse model. To quantify cyclopurine lesions in this model, we modified our original ELISA method for cyclo-dA quantification and increased its sensitivity. The improved ELISA revealed that cyclo-dA lesions accumulate with age in the brain tissues of *Xpa*$^{-/-}$ and of wt mice, but there were significantly more cyclo-dA lesions in *Xpa*$^{-/-}$ mice than in wt mice at 6, 24 and 29 months of age. These findings are consistent with the long-standing hypothesis that the age-dependent accumulation of endogenous cyclopurine lesions in the brain may be critical for XP neurological disease.

Conflict of interest

The authors declare that there are no conflicts of interest.

Acknowledgements

We thank Dr. Philip J. Brooks (NIH) for encouragement. This work was supported by JSPS KAKENHI (Ministry of Education, Culture, Sports, Science and Technology of Japan) [JP26550042, JP16H02958 to T.M.; JP26462460 to H.N.; JP16K12600 to S.S.].

References

[1] J.H. Hoeijmakers, Genome maintenance mechanisms for preventing cancer, Nature 411 (2001) 366–374.
[2] E.C. Friedberg, How nucleotide excision repair protects against cancer, Nat. Rev. Cancer 1 (2001) 22–33.
[3] K.H. Kraemer, M.M. Lee, J. Scotto, Xeroderma pigmentosum. Cutaneous, ocular, and neurologic abnormalities in 830 published cases, Arch. Dermatol. 123 (1987) 241–250.
[4] H. van Steeg, K.H. Kraemer, Xeroderma pigmentosum and the role of UV-induced DNA damage in skin cancer, Mol. Med. Today 5 (1999) 86–94.
[5] K.H. Kraemer, N.J. Patronas, R. Schiffmann, B.P. Brooks, D. Tamura, J.J. DiGiovanna, Xeroderma pigmentosum, trichothiodystrophy and Cockayne syndrome: a complex genotype-phenotype relationship, Neuroscience 145 (2007) 1388–1396.
[6] P.T. Bradford, A.M. Goldstein, D. Tamura, S.G. Khan, T. Ueda, J. Boyle, K.S. Oh, K. Imoto, H. Inui, S. Moriwaki, S. Emmert, K.M. Pike, A. Raziuddin, T.M. Plona, J.J. DiGiovanna, M.A. Tucker, K.H. Kraemer, Cancer and neurologic degeneration in xeroderma pigmentosum: long term follow-up characterises the role of DNA repair, J. Med. Genet. 48 (2011) 168–176.
[7] J.J. DiGiovanna, K.H. Kraemer, Shining a light on xeroderma pigmentosum, J. Invest. Dermatol. 132 (2012) 785–796.
[8] Y. Hirai, Y. Kodama, S. Moriwaki, A. Noda, H.M. Cullings, D.G. Macphee, K. Kodama, K. Mabuchi, K.H. Kraemer, C.E. Land, N. Nakamura, Heterozygous individuals bearing a founder mutation in the XPA DNA repair gene comprise nearly 1% of the Japanese population, Mutat. Res. 601 (2006) 171–178.
[9] C. Nishigori, E. Nakano, T. Masaki, R. Ono, S. Takeuchi, M. Tsujimoto, T. Ueda, Characteristics of xeroderma pigmentosum in Japan: lessons from two clinical surveys and measures for patient care, Photochem. Photobiol. 95 (2019) 140–153.
[10] A.D. Andrews, S.F. Barrett, J.H. Robbins, Xeroderma pigmentosum neurological abnormalities correlate with colony-forming ability after ultraviolet radiation, Proc. Natl. Acad. Sci. U.S.A. 75 (1978) 1984–1988.
[11] I. Rapin, Y. Lindenbaum, D.W. Dickson, K.H. Kraemer, J.H. Robbins, Cockayne syndrome and xeroderma pigmentosum, Neurology 55 (2000) 1442–1449.
[12] J.H. Robbins, R.A. Brumback, M. Mendiones, S.F. Barrett, J.R. Carl, S. Cho, M.B. Denckla, M.B. Ganges, L.H. Gerber, R.A. Guthrie, J. Meer, A.N. Moshell, R.J. Polinsky, P.D. Ravin, B.C. Sonies, R.E. Tarone, Neurological disease in xeroderma pigmentosum. Documentation of a late onset type of the juvenile onset form, Brain 114 (1991) 1335–1361.
[13] M. Itoh, M. Hayashi, K. Shioda, M. Minagawa, F. Isa, K. Tamagawa, Y. Morimatsu, M. Oda, Neurodegeneration in hereditary nucleotide repair disorders, Brain Dev. 21 (1999) 326–333.
[14] E.F. Fang, M. Scheibye-Knudsen, L.E. Brace, H. Kassahun, T. SenGupta, H. Nilsen, J.R. Mitchell, D.L. Croteau, V.A. Bohr, Defective mitophagy in XPA via PARP1 hyperactivation and NAD^+/SIRT1 reduction, Cell 157 (2014) 882–896.
[15] P.J. Brooks, The cyclopurine deoxynucleosides: DNA repair, biological effects, mechanistic insights, and unanswered questions, Free Radic. Biol. Med. 107 (2017) 90–100.
[16] P.J. Brooks, D.S. Wise, D.A. Berry, J.V. Kosmoski, M.J. Smerdon, R.L. Somers, H. Mackie, A.Y. Spoonde, E.J. Ackerman, K. Coleman, R.E. Tarone, J.H. Robbins, The oxidative DNA lesion 8,5'-(*S*)-cyclo-2'-deoxyadenosine is repaired by the nucleotide excision repair pathway and blocks gene expression in mammalian cells, J. Biol. Chem. 275 (2000) 22355–22362.
[17] I. Kuraoka, C. Bender, A. Romieu, J. Cadet, R.D. Wood, T. Lindahl, Removal of oxygen free-radical-induced 5',8-purine cyclodeoxynucleosides from DNA by the nucleotide excision-repair pathway in human cells, Proc. Natl. Acad. Sci. U.S.A. 97 (2000) 3832–3837.
[18] C. Marietta, H. Gulam, P.J. Brooks, A single 8,5'-cyclo-2'-deoxyadenosine lesion in a TATA box prevents binding of the TATA binding protein and strongly reduces transcription in vivo, DNA Repair (Amst.) 1 (2002) 967–975.
[19] P.J. Brooks, The case for 8,5'-cyclopurine-2'-deoxynucleosides as endogenous DNA lesions that cause neurodegeneration in xeroderma pigmentosum, Neuroscience 145 (2007) 1407–1417.
[20] P.J. Brooks, The 8,5'-cyclopurine-2'-deoxynucleosides: Candidate neurodegenerative DNA lesions in xeroderma pigmentosum, and unique probes of transcription and nucleotide excision repair, DNA Repair (Amst.) 7 (2008) 1168–1179.
[21] C. You, X. Dai, B. Yuan, J. Wang, P.J. Brooks, L.J. Niedernhofer, Y. Wang, A quantitative assay for assessing the effects of DNA lesions on transcription, Nat. Chem. Biol. 8 (2012) 817–822.
[22] P. Jaruga, M. Dizdaroglu, 8,5'-Cyclopurine-2'-deoxynucleosides in DNA: mechanisms of formation, measurement, repair and biological effects, DNA Repair (Amst.) 7 (2008) 1413–1425.
[23] T. Iwamoto, P.J. Brooks, T. Nishiwaki, K. Nishimura, N. Kobayashi, S. Sugiura, T. Mori, Quantitative and *in situ* detection of oxidatively generated DNA damage 8,5'-cyclo-2'-deoxyadenosine using an immunoassay with a novel monoclonal antibody, Photochem. Photobiol. 90 (2014) 829–836.
[24] C. Chatgilialoglu, C. Ferreri, M.A. Terzidis, Purine 5',8-cyclonucleoside lesions: chemistry and biology, Chem. Soc. Rev. 40 (2011) 1368–1382.
[25] N. Belmadoui, F. Boussicault, M. Guerra, J.L. Ravanat, C. Chatgilialoglu, J. Cadet, Radiation-induced formation of purine 5',8-cyclonucleosides in isolated and cellular DNA: high stereospecificity and modulating effect of oxygen, Org. Biomol. Chem. 8 (2010) 3211–3219.
[26] A.F. Fuciarelli, G.G. Miller, J.A. Raleigh, An immunochemical probe for 8,5'-cyclodenosine-5'-monophosphate and its deoxy analog in irradiated nucleic acids, Radiat. Res. 104 (1985) 272–283.
[27] M.A. Terzidis, C. Ferreri, C. Chatgilialoglu, Radiation-induced formation of purine lesions in single and double stranded DNA: revised quantification, Front. Chem. 3 (2015) e18.
[28] E.S. Henle, Y. Luo, W. Gassmann, S. Linn, Oxidative damage to DNA constituents by iron-mediated Fenton reactions. The deoxyguanosine family, J. Biol. Chem. 271 (1996) 21177–21186.
[29] C.R. Guerrero, J. Wang, Y. Wang, Induction of 8,5'-cyclo-2'-deoxyadenosine and 8,5'-cyclo-2'-deoxyguanosine in isolated DNA by Fenton-type reagents, Chem. Res. Toxicol. 26 (2013) 1361–1366.
[30] K. Randerath, G.-D. Zhou, R.L. Somers, J.H. Robbins, P.J. Brooks, A ^{32}P-postlabeling assay for the oxidative DNA lesion 8,5'-cyclo-2'-deoxyadenosine in mammalian tissues: evidence that four type II I-compounds are dinucleotides containing the lesion in the 3' nucleotide, J. Biol. Chem. 276 (2001) 36051–36057.
[31] K.M. Anderson, P. Jaruga, C.R. Ramsey, N.K. Gilman, V.M. Green, S.W. Rostad, J.T. Emerman, M. Dizdaroglu, D.C. Malins, Structural alterations in breast stromal and epithelial DNA: the influence of 8,5'-cyclo-2'-deoxyadenosine, Cell Cycle 5 (2006) 1240–1244.

[32] G. Kirkali, N.C. de Souza-Pinto, P. Jaruga, V.A. Bohr, M. Dizdaroglu, Accumulation of (5'*S*)-8,5'-cyclo-2'-deoxyadenosine in organs of Cockayne syndrome complementation group B gene knockout mice, DNA Repair (Amst.) 8 (2009) 274–278.
[33] J. Wang, C.L. Clauson, P.D. Robbins, L.J. Niedernhofer, Y. Wang, The oxidative DNA lesions 8,5'-cyclopurines accumulate with aging in a tissue-specific manner, Aging Cell 11 (2012) 714–716.
[34] J.A. Theruvathu, P. Jaruga, M. Dizdaroglu, P.J. Brooks, The oxidatively-induced DNA lesions 8,5'-cyclo-2'-deoxyadenosine and 8-hydroxy-2'-deoxyadenosine are strongly resistant to acid-induced hydrolysis of the glycosidic bond, Mech. Ageing Dev. 128 (2007) 494–502.
[35] R.S. Das, M. Samaraweera, M. Morton, J.A. Gascón, A.K. Basu, Stability of *N*-glycosidic bond of (5'*S*)-8,5'-cyclo-2'-deoxyguanosine, Chem. Res. Toxicol. 25 (2012) 2451–2461.
[36] P. Jaruga, Y. Xiao, B.C. Nelson, M. Dizdaroglu, Measurement of (5'*R*)- and (5'*S*)-8,5'-cyclo-2'-deoxyadenosines in DNA *in vivo* by liquid chromatography/isotope-dilution tandem mass spectrometry, Biochem. Biophys. Res. Commun. 386 (2009) 656–660.
[37] G. Kirkali, D. Keles, A.E. Canda, C. Terzi, P.T. Reddy, P. Jaruga, M. Dizdaroglu, G. Oktay, Evidence for upregulated repair of oxidatively induced DNA damage in human colorectal cancer, DNA Repair (Amst.) 10 (2011) 1114–1120.
[38] J. Wang, B. Yuan, C. Guerrero, R. Bahde, S. Gupta, Y. Wang, Quantification of oxidative DNA lesions in tissues of Long-Evans Cinnamon rats by capillary high-performance liquid chromatography-tandem mass spectrometry coupled with stable isotope-dilution method, Anal. Chem. 83 (2011) 2201–2209.
[39] H. Nakane, S. Takeuchi, S. Yuba, M. Saijo, Y. Nakatsu, H. Murai, Y. Nakatsuru, T. Ishikawa, S. Hirota, Y. Kitamura, Y. Kato, Y. Tsunoda, H. Miyauchi, T. Horio, T. Tokunaga, T. Matsunaga, O. Nikaido, Y. Nishimune, Y. Okada, K. Tanaka, High incidence of ultraviolet-B- or chemical-carcinogen-induced skin tumours in mice lacking the xeroderma pigmentosum group A gene, Nature 377 (1995) 165–168.
[40] M.A. Terzidis, C. Chatgilialoglu, An ameliorative protocol for the quantification of purine 5',8-cyclo-2'- deoxynucleosides in oxidized DNA, Front. Chem. 3 (2015) e47.
[41] M.G. Krokidis, M.A. Terzidis, E. Efthimiadou, S.-K. Zervou, G. Kordas, K. Papadopoulos, A. Hiskia, D. Kletsas, C. Chatgilialoglu, Purine 5',8-cyclo-2'-deoxynucleoside lesions: formation by radical stress and repair in human breast epithelial cancer cells, Free Radic. Res. 51 (2017) 470–482.
[42] S.Q. Gregg, A. Rasile Robinson, L.J. Niedernhofer, Physiological consequences of defects in ERCC1-XPF DNA repair endonuclease, DNA Repair (Amst.) 10 (2011) 781–791.
[43] P.J. Brooks, DNA repair in neural cells: basic science and clinical implications, Mutat. Res. 509 (2002) 93–108.
[44] H. Nakane, S. Hirota, P.J. Brooks, Y. Nakabeppu, Y. Nakatsu, Y. Nishimune, A. Iino, K. Tanaka, Impaired spermatogenesis and elevated spontaneous tumorigenesis in xeroderma pigmentosum group A gene (*Xpa*)-deficient mice, DNA Repair (Amst.) 7 (2008) 1938–1950.
[45] A. de Vries, C.T.M. van Oostrom, F.M.A. Hofhuis, P.M. Dortant, R.J.W. Berg, F.R. de Gruijl, P.W. Wester, C.F. van Kreijl, P.J.A. Capel, H. van Steeg, S.J. Verbeek, Increased susceptibility to ultraviolet-B and carcinogens of mice lacking the DNA excision repair gene XPA, Nature 377 (1995) 169–173.
[46] A. de Vries, H. van Steeg, *Xpa* knockout mice, Semin. Cancer Biol. 7 (1996) 229–240.
[47] T. Mimaki, N. Itoh, J. Abe, T. Tagawa, K. Sato, H. Yabuuchi, H. Takebe, Neurological manifestations in xeroderma pigmentosum, Ann. Neurol. 20 (1986) 70–75.
[48] H. Shinomiya, D. Yamashita, T. Fujita, E. Nakano, G. Inokuchi, S. Hasegawa, N. Otsuki, C. Nishigori, K.-I. Nibu, Hearing dysfunction in *Xpa*-deficient mice, Front. Aging Neurosci. 9 (2017) e19.
[49] T. Nouspikel, P.C. Hanawalt, Terminally differentiated human neurons repair transcribed genes but display attenuated global DNA repair and modulation of repair gene expression, Mol. Cell. Biol. 20 (2000) 1562–1570.
[50] A. Yamamoto, Y. Nakamura, N. Kobayashi, T. Iwamoto, A. Yoshioka, H. Kuniyasu, T. Kishimoto, T. Mori, Neurons and astrocytes exhibit lower activities of global genome nucleotide excision repair than do fibroblasts, DNA Repair (Amst.) 6 (2007) 649–657.
[51] G. Xu, G. Spivak, D.L. Mitchell, T. Mori, J.R. McCarrey, C.A. McMahan, R.B. Walter, P.C. Hanawalt, C.A. Walter, Nucleotide excision repair activity varies among murine spermatogenic cell types, Biol. Reprod. 73 (2005) 123–130.
[52] L.F.Z. Batista, B. Kaina, R. Meneghini, C.F.M. Menck, How DNA lesions are turned into powerful killing structures: insights from UV-induced apoptosis, Mutat. Res. 681 (2009) 197–208.
[53] G.K. Michalopoulos, Liver regeneration, J. Cell. Physiol. 213 (2007) 286–300.
[54] Y. Yu, C.R. Guerrero, S. Liu, N.J. Amato, Y. Sharma, S. Gupta, Y. Wang, Comprehensive assessment of oxidatively induced modifications of DNA in a rat model of human Wilson's disease, Mol. Cell Proteomics 15 (2016) 810–817.